FULL PAPERS

Magnetic Resonance in Medicine 56:965–970 (2006)

Localized Short-Echo-Time Proton MR Spectroscopy With Full Signal-Intensity Acquisition

Vladimír Mlynárik, Giulio Gambarota, Hanne Frenkel, and Rolf Gruetter*

We developed a short-echo-time (TE) sequence for proton localized spectroscopy by combining a 1D add-subtract scheme with a doubly slice-selective spin-echo (SE) sequence. The sequence preserves the full magnetization available from the selected volume of interest (VOI). By reducing the number of radiofrequency (RF) pulses acting on transverse magnetization, we were able to minimize the TE to the level that is achievable with the stimulated echo acquisition mode (STEAM) technique, and also gained a twofold increase in sensitivity. The use of an adiabatic pulse in the add-subtract localization improved the efficiency of excitation in spatially inhomogeneous RF fields, which are frequently encountered at high magnetic fields. The localization performance and sensitivity gains of this method, which is termed SPin ECho, full Intensity Acquired Localized (SPECIAL) spectroscopy, were demonstrated in vivo in rat brains. In conjunction with spectroscopic imaging, a 2-μl spatial resolution was accomplished with a signal-to-noise ratio (SNR) above 30, which is usually sufficient for reliable quantification of a large number of metabolites (neurochemical profile). Magn Reson Med 56:965–970, 2006. © 2006 Wiley-Liss, Inc.

Key words: proton magnetic resonance localized spectroscopy; spectroscopic imaging; short echo time; rat brain; full signal intensity

When short echo times (TEs) are used in localized proton spectroscopy, distortion of spectral multiplets due to J-evolution can be minimized, which facilitates the detection and quantitation of many important metabolites, such as glutamine, glutamate, γ-aminobutyrate, aspartate, and myo-inositol. The signals are also minimally affected by transverse relaxation, which further improves the reliability of quantification.

Localized spectroscopy has been largely based on stimulated-echo acquisition mode (STEAM) (1) or point-resolved spectroscopy (PRESS) methods (2). The STEAM sequence benefits from lower chemical shift displacement error due to the larger bandwidth of its 90° RF pulses at a given peak RF power compared to the 180° pulses used in PRESS. Moreover, the performance of the STEAM sequence is less sensitive to B_1 inhomogeneity. The short-TE STEAM sequence does not require strong spoiling gradients, because unwanted coherence pathways (except for the free induction decay (FID) formed by the last slice-selective RF pulse) are efficiently suppressed by the spoiling gradient pulse in the mixing time (TM) period. These favorable circumstances permitted STEAM spectra and STEAM-based spectroscopic imaging data to be obtained in rats with TEs as short as 1 ms (3) and 2 ms (4), respectively. Values below 10 ms have been used to obtain STEAM spectra from humans at different magnetic fields: 5 ms (5) and 6 ms (6) at 1.5 T, 6.8 ms at 3 T (7), 5 ms at 4 T (8), and 6 ms at 7 T (9).

In theory, the PRESS technique can obtain full signal intensity from the selected volume of interest (VOI). In practice, however, the two slice-selective 180° pulses used in PRESS have a smaller bandwidth than the pulses in STEAM, which is often accentuated by RF peak power limitations. The PRESS sequence is intrinsically sensitive to B_1 variation, which can limit the sensitivity gains achievable, especially at high magnetic fields. In addition, the dephasing of unwanted signals created by the slice-selective RF pulses requires significant gradient spoiling, which increases the minimum TE. Recent studies have used PRESS-based single-voxel spectroscopy and spectroscopic imaging with a TE of 6 ms in rats (10), and PRESS localized spectroscopy with a TE of 8–10 ms in humans (11).

Using a 9.4-Tesla system with substantially improved gradient and eddy-current performance, we sought to demonstrate the feasibility of full-sensitivity localization with a TE comparable to that of STEAM under similar experimental conditions.

MATERIALS AND METHODS

ANIMALS

Experiments were performed on healthy male Sprague Dawley rats with a mean weight of 285 g. The animals were injected with 0.4 mg/kg midazolam intraperitoneally, and were then intubated and artificially ventilated with a mixture of N_2O/O_2 (3:1) and isoflurane (1.5%). Body temperature was maintained at 37.5°C by circulating the body with warm air. All procedures involving animals conformed to local and federal guidelines and were approved by the local ethics committee.

All measurements were performed on a Varian INOVA spectrometer (Varian, Palo Alto, CA, USA) interfaced to a 9.4-Tesla, actively-shielded magnet with a 31-cm horizontal bore (Magnex Scientific, Abingdon, UK), 2.8 ppm ho-

Laboratory of Functional and Metabolic Imaging, École Polytechnique Fédérale de Lausanne, Lausanne, Switzerland.

Grant sponsors: Centre d'Imagerie BioMedicale of the UNIL, EPFL, UNIGE, CHUV and HUG; Leenaards Foundation; Jeantet Foundation.

*Correspondence to: Prof. Rolf Gruetter, Laboratory of Functional and Metabolic Imaging, École Polytechnique Fédérale de Lausanne, Station 6, CH-1015 Lausanne, Switzerland. E-mail: rolf.gruetter@epfl.ch

Received 6 April 2006; revised 11 July 2006; accepted 11 July 2006.
DOI 10.1002/mrm.21043
Published online 21 September 2006 in Wiley InterScience (www.interscience.wiley.com).

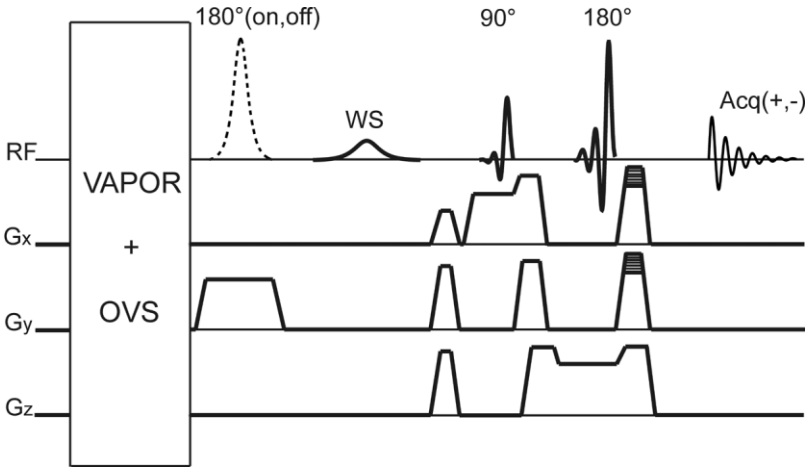

FIG. 1. Scheme of the hybrid pulse sequence. The first 180° pulse is adiabatic and is applied in alternate scans, together with alternating the phase of the receiver. Phase encoding is applied for spectroscopic imaging only. WS represents an additional water suppression pulse.

mogeneity over a 14-cm-diameter spherical volume, and a 12-cm inner diameter, actively-shielded gradient set (400 mT/m in 120 μs). Eddy currents were minimized to below 0.01% using time-dependent quantitative eddy-current field mapping (12). First- and second-order shims were adjusted for selected VOIs using an EPI version of FASTMAP (13). An in-house-built quadrature transmit/receive surface coil with two geometrically decoupled 14-mm-diameter single loops resonating at 400 MHz was used.

Pulse Sequence

The new hybrid pulse sequence (Fig. 1) is based on a combination of the 1D image-selected in vivo spectroscopy (ISIS) (14) technique and a slice-selective spin-echo (SE) sequence. In the localized spectroscopy mode, localization in the vertical direction perpendicular to the plane of the coil was achieved by application of a 2-ms slice-selective full-passage adiabatic pulse (with a bandwidth of 10 kHz) in alternate scans, followed by a spoiling gradient. Then a SE sequence was applied using 0.5-ms 90° and 180° asymmetric slice-selective pulses (3,10) in both directions parallel to the coil plane, corresponding to a peak B_1 of 3.35 and 9.90 kHz. The bandwidths of the 0.5-ms 90° and 180° pulses were 13.5 kHz and 11.6 kHz, respectively. The signal was added in odd scans and subtracted in even scans, corresponding to the application of the adiabatic inversion pulse in the add-subtract scheme as in 1D ISIS. Both asymmetric pulses had excellent frequency selectivity, and the asymmetric 90° pulse shortened the minimum TE. The shape of the 180° pulse was not critical, since its full duration contributed to the TE and its shape was selected according to time periods necessary for the spoiling and refocusing gradient pulses. Using the described pulse sequence elements, the minimum TE achieved was 2.2 ms with a 0.5-ms 180° pulse, and 2.7 ms with a 1-ms

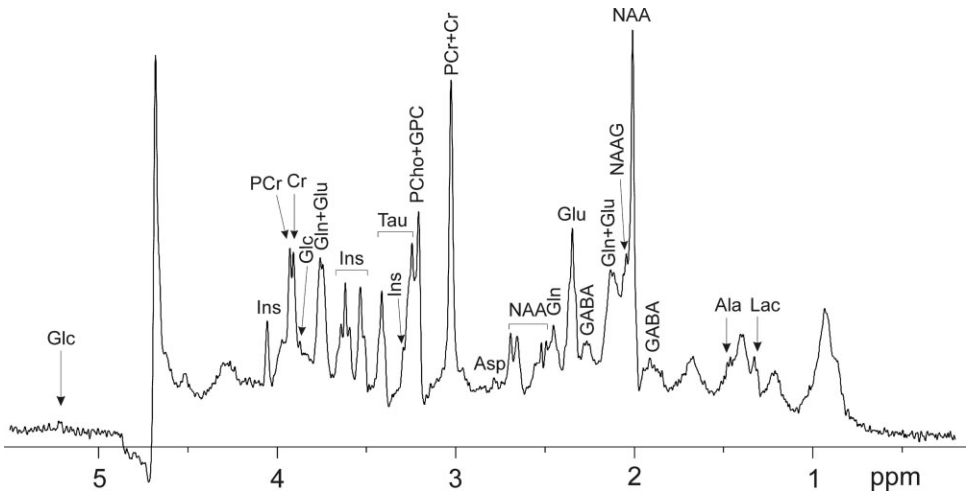

FIG. 2. A proton spectrum measured with the hybrid sequence from a volume of $4 \times 3 \times 4$ mm^3 comprising the frontal cortex and putamen of the rat brain (TR = 4000 ms, TE = 2.2 ms, and number of scans = 160). A shifted Gaussian function (gf = 0.12, gfs = 0.08) was used for modest resolution enhancement. No baseline correction or postprocessing for water signal removal was applied. Ala = alanine, Asp = aspartate, Cr = creatine, GABA = γ-aminobutyrate, Glc = glucose, Gln = glutamine, Glu = glutamate, GPC = glycerophosphocholine, Ins = myo-inositol, Lac = lactate, NAA = N-acetylaspartate, NAAG = N-acetylaspartylglutamate, PCr = phosphocreatine, Tau = taurine.

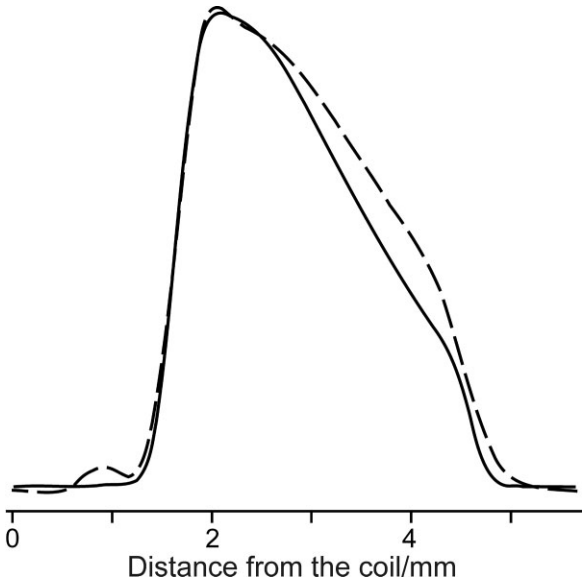

FIG. 3. Profiles of the VOI ($4 \times 3 \times 4$ mm^3) in the direction perpendicular to the RF coil plane (parallel to the Y-axis). A phantom filled with water was measured using the STEAM (dashed line) and hybrid (solid line) sequences. The signal intensity of the profile excited by STEAM was multiplied by 2.

180° pulse, respectively. For this pulse sequence we propose the term SPin ECho, full Intensity Acquired Localized (SPECIAL) spectroscopy.

In the rat studies the voxel size ranged between 23 and 62 μL, the repetition time (TR) was 4 s, and a spectral width of 5000 Hz was collected into 4096 complex points with an acquisition time of 0.82 s. The number of accumulations was 160 or 240. Data processing consisted of zero-filling up to 16-k data points, Gaussian weighting of the FID, Fourier transformation, and zero- and first-order phase correction.

Water signal suppression was accomplished by a series of seven 25-ms asymmetric variable power RF pulses with optimized relaxation delays (VAPOR) as described previously (3). The water suppression pulses were interleaved with outer volume saturation (OVS) consisting of three modules of 1.2-ms adiabatic pulses. The bandwidths of the water suppression pulses and the OVS pulses were 270 Hz and 35 kHz, respectively. To further improve the efficiency of water suppression, another frequency-selective saturation pulse (15 ms Gaussian, bandwidth = 180 Hz) was added in the delay between the adiabatic slice-selective inversion pulse and the SE modules.

In the spectroscopic imaging mode, a voxel of $4 \times 4 \times 2$ mm^3 was localized in the transverse (XY) plane. Due to the extended dimension in the vertical (Y) direction, a 1.0-ms 180° refocusing pulse was used, which led to a TE of 2.7 ms. The excited voxel was further encoded in the X and Y directions with 32×32 steps using a field of view (FOV) of 32×32 mm^2, resulting in a nominal voxel size of 2.0 μL. For each phase-encoding step 2048 complex points were acquired in the spectral domain. With a TR of 3.5 s and two scans acquired for each phase-encoding step, the total scan time was about 2 hr.

The processing of the spectroscopic imaging data involved 2D spatial Fourier transformation without any weighting of the *k*-space. Then localized FIDs were zero-filled to 8 K, Gaussian weighted, Fourier transformed, and zero- and first-order phase-corrected. A region of 7×7 voxels comprising the excited region of the rat brain was then overlaid on an anatomical image. The image was obtained by a fast SE technique (TR = 2 s, TE_{ef} = 48 ms, and eight echoes per scan) using a FOV of 32 mm × 32 mm and a matrix size of 256 × 128 data points.

RESULTS

Figure 2 illustrates the performance achieved with this sequence. Notably, no artifacts from extravoxel water coherences or extracerebral lipid signals were discernible, and the amplitude of the residual water signal was similar to the amplitudes of the metabolite signals. The slice profiles of the same VOI excited with both STEAM and the hybrid sequence in the direction perpendicular to the coil plane (i.e., in the direction of the maximum B_1 field gradient) are depicted in Fig. 3. The actual width of the profile excited by the amplitude-modulated pulse in the STEAM sequence was slightly larger and depended on the fine adjustment of the slice-selection pulse amplitude (not shown). In contrast, the width of the profile achieved with the hybrid sequence should not depend on the amplitude of the adiabatic pulse used in the Y direction when it is above the adiabaticity threshold (15).

We assessed the gain in sensitivity achieved with the new scheme by comparing spectra measured with STEAM and the hybrid sequence using an identical number of scans, TR, TE, and VOI (see Fig. 4). The difference spectrum was calculated with the absolute intensity of the hybrid sequence scaled by a factor of 0.535, consistent with an almost twofold gain in sensitivity.

To assess the potential influence of using an add-subtract scheme for localization, and to demonstrate the benefit of higher signal intensity obtained by the hybrid sequence, we acquired a chemical shift image in two rats. Figure 5 shows a high-resolution spectroscopic image with 2 μL voxel size that is devoid of any discernible extracranial fat signal. The actual width of the excited region is slightly larger than 4 mm due to the frequency profile of the 90° excitation pulse. On the other hand, its vertical dimension is limited by the sensitive volume of the surface coil. The high signal intensity enabled us to obtain spectra from 2-μl voxels in 2 hr with a signal-to-noise ratio (SNR) greater than 30 (Fig. 5), which is typically deemed sufficient for obtaining a full neurochemical profile.

Using the same basis set of metabolite spectra, we determined absolute concentrations of metabolites using LC-Model (16) and compared them using the spectra obtained by single-voxel spectroscopy from three rats measured with both methods from the same VOI and using identical timing and averaging. The voxel sizes were 23, 48, and 62 μL, respectively. On average, the mean concentrations obtained by the hybrid sequence were in excellent agreement with those calculated from the STEAM spectra (Table 1). When the concentrations obtained by SPECIAL vs. the concentrations obtained by STEAM were plotted, this function was indistinguishable from the identity line.

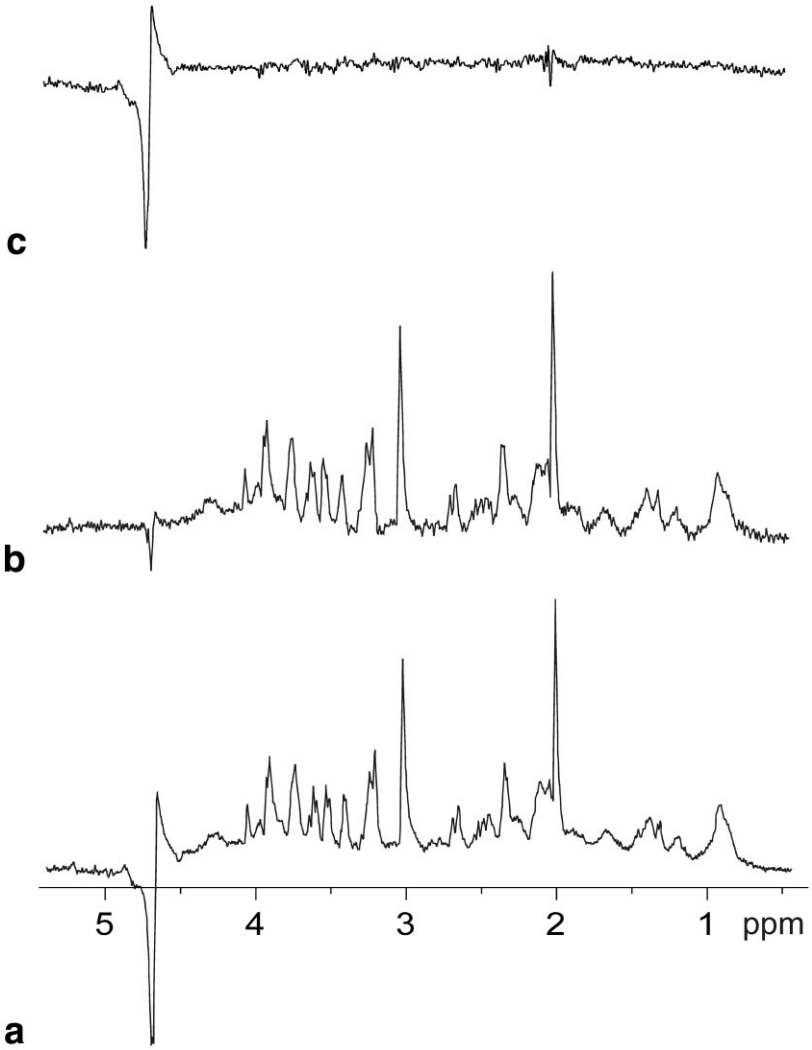

FIG. 4. Spectra measured from the same VOI (50 μL) using the hybrid sequence (**a**) and STEAM (**b**). The absolute signal intensities in the spectrum measured by the hybrid sequence were multiplied by 0.535. The same TE (2.7 ms), TR (4 s), number of scans (240), and data processing (gf = 0.12, gfs = 0.06) were used. The difference spectrum (**c**) was calculated by subtracting the STEAM spectrum from that of the hybrid sequence.

DISCUSSION

The proposed hybrid localization sequence uses only one refocusing pulse, which shortens the minimum achievable TE and thus allows short TEs comparable to those attainable by STEAM. At the same time, the third spatial dimension is selected with an adiabatic 180° pulse, the potential transverse magnetization of which can be efficiently removed by the spoiling gradient in the time delay between the ISIS and SE modules. This delay does not contribute to the overall TE of the sequence since the magnetization is conserved along the static magnetic field. The period between the ISIS and SE modules is in many ways analogous to the TM period of the STEAM sequence, and can be used for an additional water suppression pulse, as was done in the present implementation.

The use of an adiabatic pulse for slice selection in one spatial direction reduces the B_1 dependence of the obtained localized signal. Inhomogeneous RF fields are present in experiments that use surface coil excitation, and at very high magnetic fields. The use of the adiabatic pulse guarantees homogeneous inversion of all the magnetization available in the selected VOI, and thus further minimizes signal loss. In effect, the "non-adiabatic" part of the localization sequence $(\theta - 2\theta)$ has a B_1 dependence that theoretically is identical to that of STEAM $(\theta - \theta - \theta)$ (17), i.e., $\sin\theta \cdot \sin^2(2\theta/2) = \sin^3\theta$. Consequently, our experiments showed a close to twofold increase in the SNR obtained with the hybrid sequence compared to STEAM, even when a surface coil was used as a transceiver. The observed small loss in signal intensity (on the order of a few percent) can be explained by the mismatch in the actual voxel dimensions selected by the amplitude-modulated pulse in STEAM, and by the adiabatic pulse in the hybrid pulse sequence (Fig. 3).

The described hybrid technique requires a minimum of two scans for the add-subtract scheme used for localization of the third dimension. Great care was used to minimize any potential contribution from outside the VOI with additional OVS. The resulting quality of localization was evaluated using spectroscopic imaging (Fig. 5). The degree of water suppression obtained using VAPOR combined with the OVS scheme (3) was excellent. The height of the residual water signal was usually comparable to those of NAA and creatine, which is deemed sufficient for many applications.

The spectroscopic imaging experiment using our SPECIAL hybrid sequence provided a series of high-SNR spec-

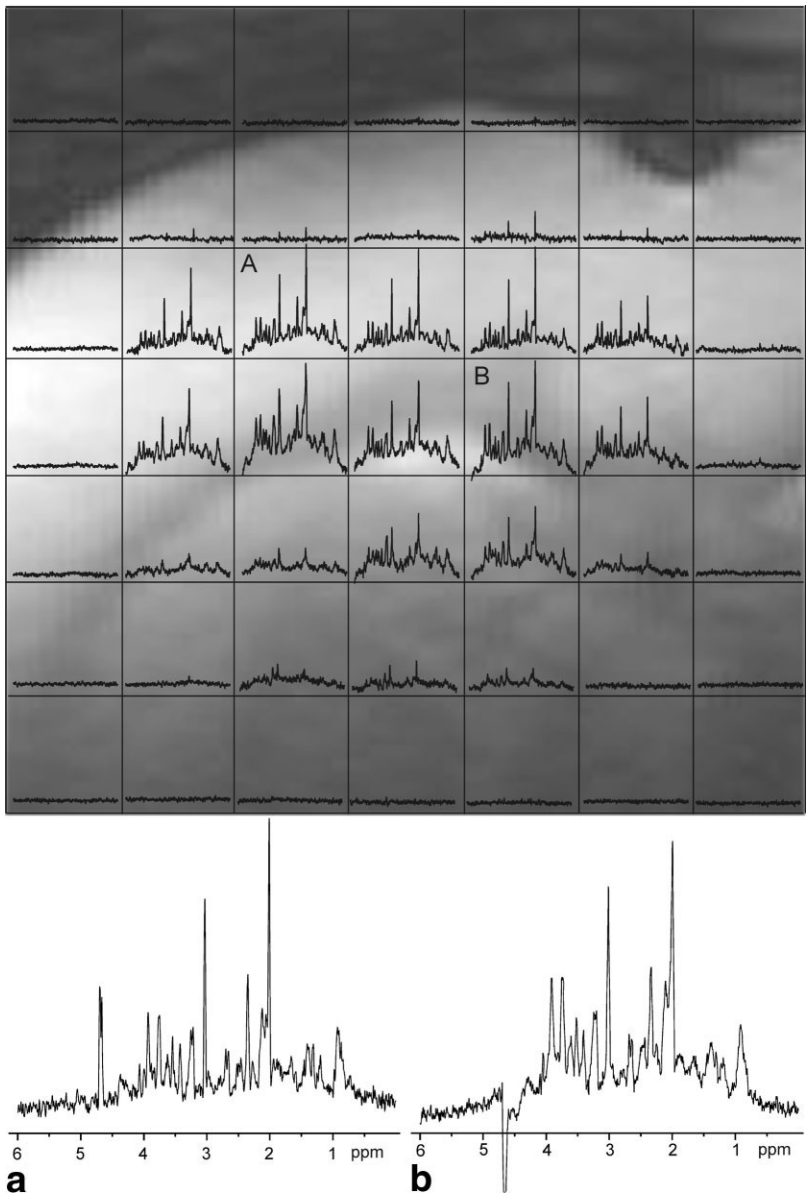

FIG. 5. High-resolution spectroscopic image of a rat brain. The matrix of short-TE (2.7 ms) proton spectra corresponds to a nominal spatial resolution of $1 \times 1 \times 2$ mm^3 within an excited volume of $4 \times 4 \times 2$ mm^3 encoded in the transverse (XY) plane. Spectrum **a** was taken from the frontal cortex (voxel A), and spectrum **b** was localized in the putamen (voxel B). Note that the traces from the voxels comprising the scalp do not show any signals of lipids.

tra with extremely high spatial resolution. Due to the variation in sensitivity of the surface coil, absolute signal intensities decreased with the distance from the coil plane. In this high-resolution spectroscopic imaging experiment, rectangular *k*-space sampling and a large FOV were used. This led to a measurement time of about 2 hr. It may be possible to reduce the measurement time by using circularly reduced *k*-space sampling (18) or a smaller FOV with fewer phase-encoding steps, which would yield substantial reductions in measurement time with concomitant losses in sensitivity. It should thus be possible to collect high-resolution chemical shift images within 1 hr with minimal loss in sensitivity owing to the square-root law of signal averaging.

Since the TEs of the STEAM and hybrid sequences were essentially the same, evolution of the J-coupled multiplets was considered negligible and the contribution of underlying macromolecule resonances was very similar. This is also evident in Fig. 4, which shows that the spectra acquired by the two methods were almost identical. An important consequence was that the calculation of metabolite concentrations by LCModel was performed with the same basis set, which considerably simplified the implementation of quantitation by obviating the need to collect a different set of basis spectra. An additional benefit of acquiring spectra at very short TEs is the fact that J-evolution need not be taken into account to generate the basis set. In other words, spin simulations used for short-echo STEAM (9,19) can also be used in conjunction with the proposed sequence.

The development of a full signal-intensity protocol with the shortest TE possible should also be beneficial for human applications of proton localized spectroscopy. As shown in a previous study, modulation of J-coupled multiplets can distort multiplet shapes even at TEs of 10–20 ms (3). When the proposed localized spectroscopy sequence is transferred to a human scanner with lower RF peak power and weaker gradients, similar increases in the minimum TE are expected (by

Table 1
Comparison of Concentrations of Metabolites Determined Using LCModel from Three Animals Measured Using STEAM and the Hybrid Sequence, Respectively, in a Paired Fashion

Metabolite	Concentration obtained from			
	STEAM		Hybrid sequence	
	Mean value (mM)	Mean CRLB[b] (mM)	Mean value (mM)	Mean CRLB (mM)
Alanine	0.3	0.2	0.3	0.1
Ascorbate	1.4	0.3	2.3	0.2
Aspartate	1.3	0.5	1.6	0.3
Creatine (Cr)	3.9	0.3	4.0	0.2
Phosphocreatine (PCr)	4.7	0.3	4.6	0.2
Cr+PCr	8.6	0.2	8.6	0.1
γ-Aminobutyrate	1.5	0.2	1.1	0.1
Glucose	2.0	0.4	1.8	0.3
Glutamine (Gln)	2.2	0.2	2.4	0.2
Glutamate (Glu)	10.3	0.3	10.3	0.2
Gln+Glu	12.5	0.3	12.6	0.2
Glutathione	0.6	0.1	0.4	0.1
Myo-inositol	6.9	0.3	6.6	0.2
Lactate[a]	1.9	0.2	1.4	0.1
N-acetylaspartate (NAA)	9.1	0.3	8.8	0.1
N-acetylaspartylglutamate (NAAG)	0.9	0.2	0.7	0.1
NAA+NAAG	10.0	0.3	9.5	0.1
Phosphocholine + glycerophosphocholine	1.0	0.2	1.1	0.2
Phosphoethanolamine	2.4	0.3	2.2	0.2
Taurine	4.7	0.2	5.0	0.2
Macromolecules	1.72	0.05	1.73	0.03

[a]Concentration of lactate varied in some experiments.
[b]Cramer-Rao lower bounds.

about 4–5 ms, as reported for short-echo STEAM), while a minimal evolution time for J-coupled spins will be retained. Hence, a human localized spectroscopy protocol based on the newly developed hybrid pulse sequence is expected to offer similar increases in the quality of the spectra and improved reliability of the calculated metabolite concentrations.

ACKNOWLEDGMENTS

This work was supported by the Centre d'Imagerie Biomedicale (CIBM) of the UNIL, EPFL, UNIGE, CHUV and HUG and the Foundations Leenaards and Louis Jeantet de Medecine.

REFERENCES

1. Frahm J, Merboldt KD, Hänicke W. Localized proton spectroscopy using stimulated echoes. J Magn Reson 1987;72:502–508.
2. Bottomley PA. Spatial localization in NMR spectroscopy in vivo. Ann NY Acad Sci 1987;508:333–348.
3. Tkáč I, Starčuk Z, Choi IY, Gruetter R. In vivo ^{1}H NMR spectroscopy of rat brain at 1 ms echo time. Magn Reson Med 1999;41:649–656.
4. Liimatainen T, Hakumäki J, Tkáč I, Gröhn O. Ultra-short echo time spectroscopic imaging in rats: implications for monitoring lipids in glioma gene therapy. NMR Biomed 2006;19:554–559.
5. Seeger U, Klose U, Seitz D, Nägele T, Lutz O, Grodd W. Proton spectroscopy of human brain with very short echo time using high gradient amplitudes. Magn Reson Imaging 1998;16:55–62.
6. Knight-Scott J, Shanbhag DD, Dunham SA. A phase rotation scheme for achieving very short echo times with localized stimulated echo spectroscopy. Magn Reson Imaging 2005;23:871–876.
7. Mlynárik V, Gruber S, Starčuk Z, Starčuk Jr Z, Moser E. Very short echo time proton MR spectroscopy of human brain with a standard transmit/receive surface coil. Magn Reson Med 2000;44:964–967.
8. Öz G, Terpstra M, Tkáč I, Aia P, Lowary J, Tuite PJ, Gruetter R. Proton MRS of the unilateral substantia nigra in the human brain at 4 tesla: detection of high GABA concentrations. Magn Reson Med 2006;55:296–301.
9. Tkáč I, Andersen P, Adriany G, Merkle H, Ugurbil K, Gruetter R. In vivo ^{1}H NMR spectroscopy of the human brain at 7 T. Magn Reson Med 2001;46:451–456.
10. Geppert C, Dreher W, Leibfritz D. PRESS-based proton single-voxel spectroscopy and spectroscopic imaging with very short echo times using asymmetric RF pulses. MAGMA 2003;16:144–148.
11. Zhong K, Ernst T. Localized in vivo human ^{1}H MRS at very short echo times. Magn Reson Med 2004;52:898–901.
12. Terpstra M, Andersen PM, Gruetter R. Localized eddy current compensation using quantitative field mapping. J Magn Reson 1998;131:139–143.
13. Gruetter R, Tkáč I. Field mapping without reference scan using asymmetric echo-planar techniques. Magn Reson Med 2000;43:319–323.
14. Ordidge RJ, Connelly A, Lohman JAB. Image-selected invivo spectroscopy (ISIS)—a new technique for spatially selective NMR-spectroscopy. J Magn Reson 1986;66:283–294.
15. Gruetter R, Boesch C, Martin E, Wüthrich K. A method for rapid evaluation of saturation factors in in vivo surface coil NMR spectroscopy using B_1-insensitive pulse cycles. NMR Biomed 1990;3:265–271.
16. Provencher SW. Estimation of metabolic concentrations from localized in vivo ^{1}H spectroscopy. Magn Reson Med 1993;30:672–679.
17. Moonen CTW, von Kienlin M, van Zijl PCM, Cohen J, Gillen J, Daly P, Wolf G. Comparison of single-shot localization methods (STEAM and PRESS) for in vivo proton NMR spectroscopy. NMR Biomed 1989;2:201–208.
18. Maudsley AA, Wu Z, Meyerhoff DJ, Weiner MW. Automated processing for proton spectroscopic imaging using water reference deconvolution. Magn Reson Med 1994;31:589–595.
19. Pfeuffer J, Juchem C, Merkle H, Nauerth A, Logothetis NK. High-field localized ^{1}H NMR spectroscopy in the anesthetized and in the awake monkey. Magn Reson Imaging 2004;22:1361–1372.